Tellus (1991), *43A*, 275–284

Baroclinic instability in a two-layer, vertically semi-infinite domain

By JOHANNES C. MÜLLER, *Atmospheric Physics ETH, Hönggerberg HPP, 8093 Zürich, Switzerland*

(Manuscript received 20 September 1989; in final form 19 February 1991)

ABSTRACT

A quasi-geostrophic two-layer system with uniform, but different, shears and stratifications in two layers is examined for the occurrence of baroclinic instability. A derived necessary condition for instability requires that the shear in the upper, semi-infinite layer does not exceed a certain value (related to the stratification). For each configuration of the basic flow, there appear two short and two long neutral modes as well as a decaying and a growing mode at intermediate wavelengths. The short neutral modes are bound to either the surface or the interface, the long neutral modes to one or other of the layers. Instability appears if the foregoing modes propagate at a similar velocity. The depth of the waves is shown to be of less importance in the framework of potential vorticity dynamics. For some configurations, the growth rates surpass those of the classical Eady problem. Finally some consideration is given to the linkage between these results and the formation of polar lows.

1. Introduction

Various extensions of the classical Eady (1949) model for baroclinic instability have been studied in the past decades, e.g., the impact of the β-effect, compressibility or meridional variations of the mean flow (see, e.g., Simmons (1979) for a review). Refinement of the vertical structure may be another way of broadening the Eady model applicability to atmospheric motions. Blumen (1979) examined this latter modification for two layers of different stratification and was able to illustrate the occurrence of short unstable waves. Some implications of a simultaneous variation of the shear in these two layers were discussed by Weng and Barcilon (1987). They also studied the impact of Ekman dissipation and surface heating on explosive cyclogenesis, and concluded that these processes did not significantly increase the maximum growth rates.

The present work follows that of Blumen (1979) with the exception that changes of potential vorticity are concentrated near the surface and in the transition zone of the layers. If these two bands are well separated their intensity is much more important than their precise forms. Therefore in this study the transition zone between the layers is represented by an interface (or pseudo-tropopause) with an infinitesimally thin sheet of potential vorticity gradient. Even though this configuration has several idealized features, it mitigates some of the unrealistic aspects of a rigid lid representation of the tropopause.

Eady's (1949) paper mentions but does not discuss a multilayer model with different stratifications. The present study allows shear variation as well. The simplicity of the present model provides an overview of the stability characteristics in this basic flow configuration and offers some explanations for qualitatively different types of wave behaviour. In particular, short wave instability and the formation of short and long neutral modes are discussed. The study relates directly to the relevance of upper layer (stratosphere) properties for instability in lower layers. Section 2 gives some details of the model formulation. Necessary and sufficient conditions for instability as well as an overview of the impact of changes in the basic flow parameters are discussed in Section 3. Section 4 examines the wave properties and vertical structures of stable and unstable modes. In a last section the results are summarized and some remarks on the applicability of the results to rapid cyclogenesis are made.

2. Model outline

The present model system describes the adiabatic, inviscid flow of a two-layer Boussinesq fluid on an f-plane. The two horizontal model layers are of uniform, but of different stratification and baroclinicity, and the upper layer is unbounded above. Two-dimensional perturbations of this basic flow configuration are considered in the quasi-geostrophic framework. A similar model but with an additional upper lid was studied extensively by Blumen (1979). In a previous study (Müller et al., 1989) a one-layer, semi-geostrophic variant of the present configuration has been examined. The structure of the basic flow field is displayed schematically in Fig. 1. The mean wind is along the x-axis and has the uniform shears $\bar{U}_z = \Lambda_1$ and Λ_2 in the lower and upper layers respectively. The Brunt-Väisälä frequencies N_1 and N_2 are also assumed constant.

Two-dimensional perturbations with zero potential vorticity are introduced in each layer. In the quasi-geostrophic framework (cf. Pedlosky (1987)), the non-dimensional perturbation streamfunction Φ obeys Laplacian equations of the form

$$\begin{Bmatrix} 1 \\ \nu^2 \end{Bmatrix} \Phi_{xx} + \Phi_{zz} = 0 \qquad \text{for} \quad \begin{cases} 0 \leqslant z \leqslant \eta \\ z \geqslant \eta, \end{cases} \tag{1}$$

where η stands for the non-dimensional height of the interface and

$$\nu \equiv N_2/N_1 \tag{2}$$

is the ratio of the Brunt-Väisälä frequencies of the upper and lower layer. The lower boundary condition follows from the linearized equation for the conservation of potential temperature at the surface:

$$\Phi_{zt} - \Phi_x = 0 \qquad \text{at} \quad z = 0, \tag{3}$$

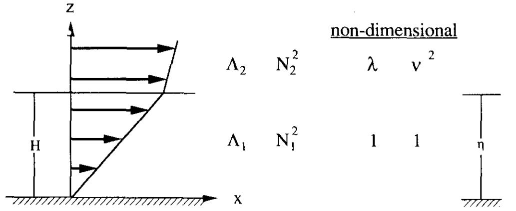

Fig. 1. Basic two-layer flow. For each layer the shear and stratification are given in dimensional and non-dimensional form. All parameters are explained in the text.

where we have assumed that the basic zonal velocity vanishes at that boundary. Due to the absence of an upper lid we demand

$$\Phi \to \text{const.} \qquad \text{for} \quad z \to \infty. \tag{4}$$

The latter condition implies that there is no vertical energy transport as $z \to \infty$ and that the northerly wind v' $(=\Phi_x)$ and the potential temperature θ' $(=\Phi_z)$ must tend to zero as $z \to \infty$. At the interface, dynamical consistency requires that the pressure and the vertical wind fields be continuous (cf. Blumen, 1979), and hence

$$\Phi|_{z=\eta^-} = \Phi|_{z=\eta^+}, \tag{5}$$

$$\nu^2(\Phi_{zt} + \eta\Phi_{zx} - \Phi_x)|_{z=\eta^-} = (\Phi_{zt} + \eta\Phi_{zx} - \lambda\Phi_x)|_{z=\eta^+}, \tag{6}$$

where

$$\lambda \equiv \Lambda_2/\Lambda_1 \tag{7}$$

denotes the ratio of the basic shears of both model layers.

To study the stability of the basic flow, consider wave-like solutions of (1) with frequency ω and horizontal wave number k. Application of the boundary and interface conditions (3–6) yields the dispersion relation:

$$\omega^2 - 2b\omega + c = 0, \tag{8}$$

where

$$b = \gamma + \frac{1}{2\nu}\frac{1 + \lambda s/(2\nu)}{1 + s/(2\nu)},$$

$$c = \frac{\gamma s - 1 + (2/\nu)[\gamma + \lambda/(2\nu)]}{1 + s/(2\nu)},$$

$$\gamma = k\eta/2, \qquad s = 2\coth(2\gamma).$$

It follows that the frequency ω depends only on the non-dimensional wave number γ (scaled by the depth of the lower layer), on the relative stratification ν and shear λ. Real solutions of (8) describe neutral modes, complex solutions correspond to growing and decaying waves with growth rate

$$\sigma = \sqrt{(c - b^2)}. \tag{9}$$

Eq. (8) recovers the special case of the classical

Eady (1949) model with a rigid lid at $z = \eta$ for $\nu = \infty$, $\lambda \neq \infty$. In the following sections baroclinic instability and some wave properties will be examined using the dispersion relation (8).

3. Stability analysis

The present system is unstable for intermediate wave lengths and stable at both ends of the spectrum. An overview of these phenomena in various basic flow configurations is given and some features of the stability behaviour are catalogued.

3.1. Necessary condition for instability

Consider first the values of (ν, λ) that will lead to baroclinic instability. A necessary condition for instability is that the meridional gradient of the basic state potential vorticity $\widehat{q_y}$ (which takes the

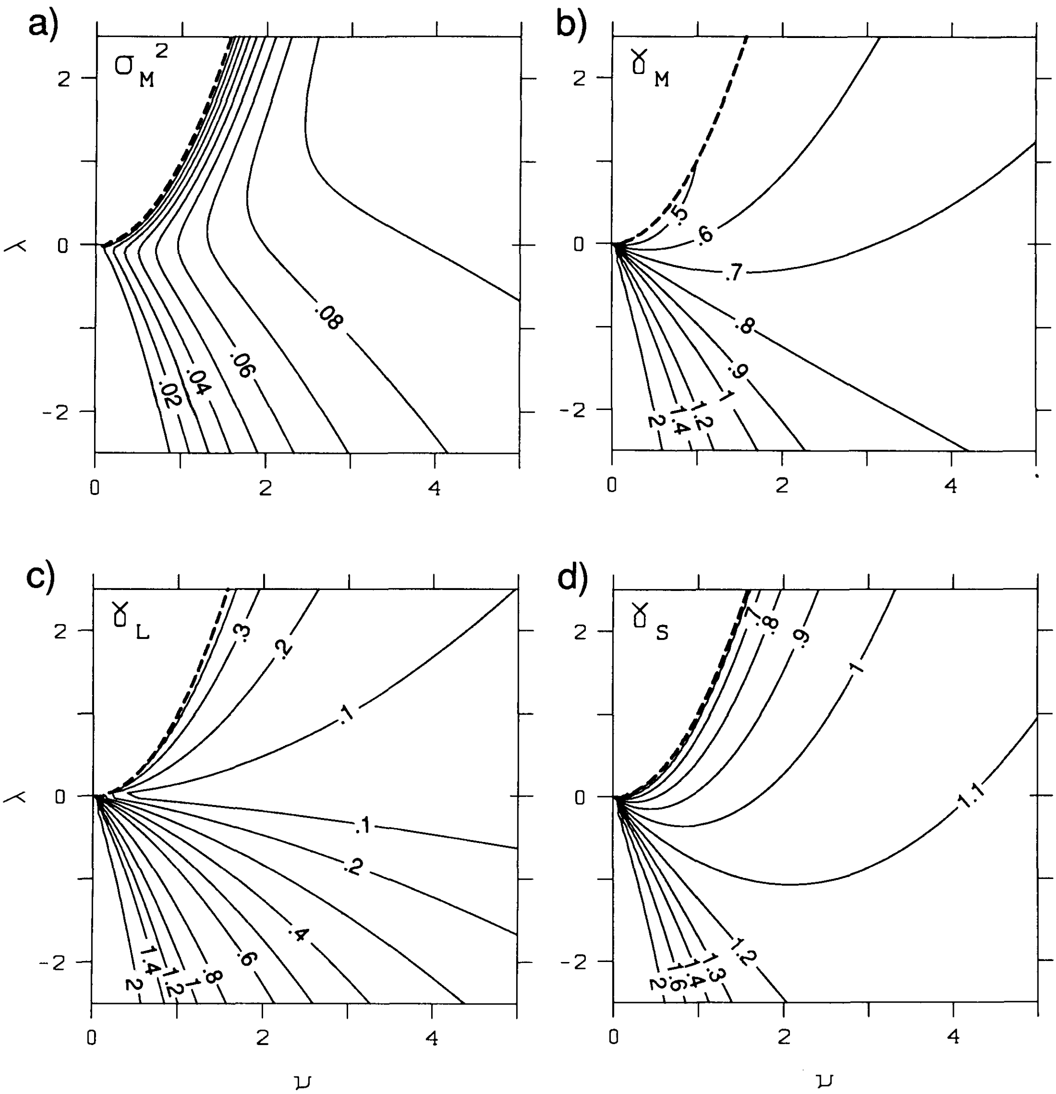

Fig. 2. Stability characteristics for varying relative shear and stratification. Shown are (a) the square of the maximum growth rate σ_M^2, (b) the corresponding wave number γ_M ($=k_M\eta/2$), and the wave numbers (c) γ_S of the short wave cut-off and (d) γ_L of the long wave cut-off. The dashed curve ($\lambda = \nu^2$) is the marginal curve.

boundary thermal pattern into account) has to change sign over the depth of the fluid (Bretherton, 1966). In the present two-layer configuration

$$\widehat{q_y} = -[\lambda/v^2 - 1]\,\delta(z-\eta) - \delta(z), \tag{10}$$

where the first term reflects the change of properties at the interface and the second the potential temperature at the surface. Here the potential vorticity derivatives near the ground and at the pseudo-tropopause have been represented by thin sheets (δ-functions). The necessary condition for baroclinic instability is

$$\lambda < v^2 \tag{11}$$

so as to allow $\widehat{q_y}$ to change sign. Hence strong positive shear in the upper layer prevents unstable modes. That implies that, for instability, the slope of the basic state isentropes has to be steeper in the lower layer than in the upper layer. Fig. 2 (see Subsection 3.2) shows that condition (11) is also sufficient for the occurrence of baroclinic instability.

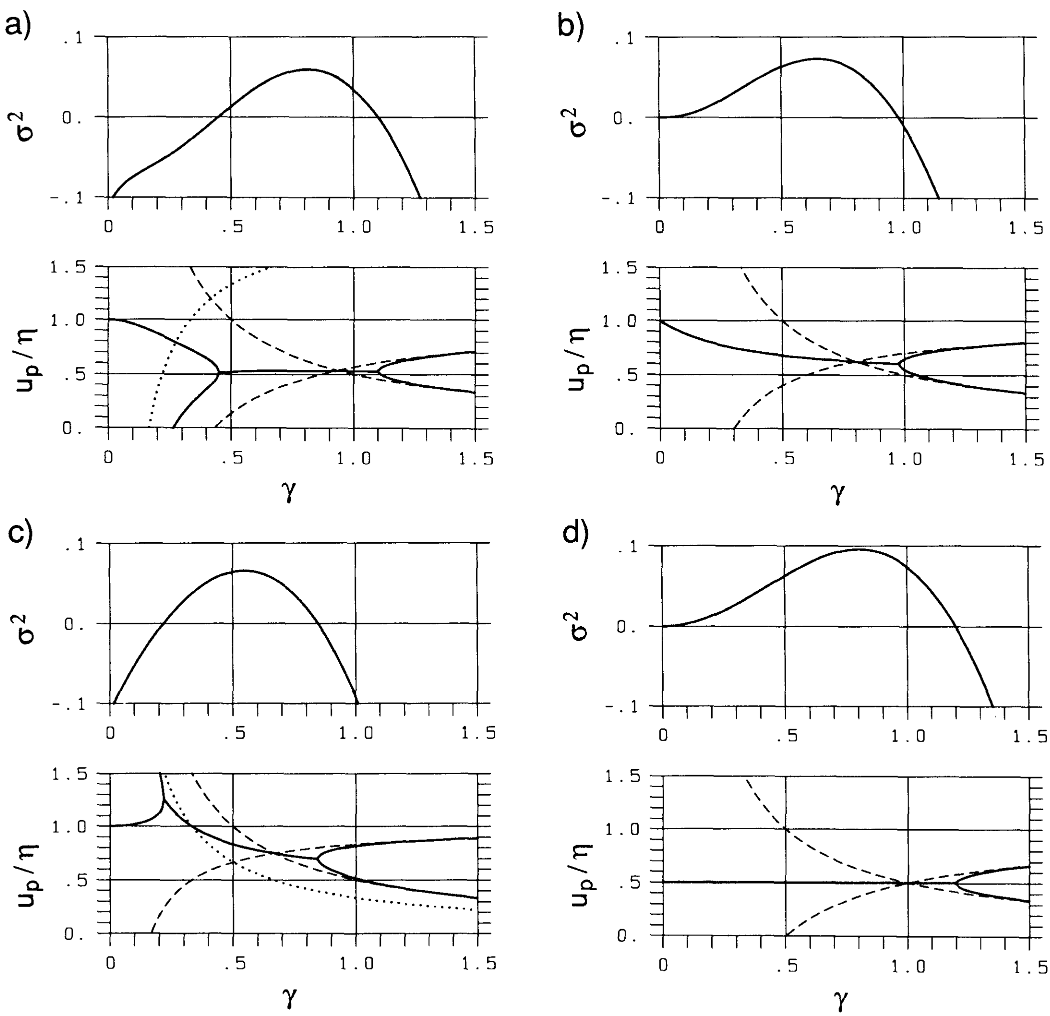

Fig. 3. Growth rate σ and phase velocities u_p as a function of the wave number γ for various configurations. In the first cases $v = 1.5$ and (a) $\lambda = -1$, (b) $\lambda = 0$ and (c) $\lambda = 1$. For comparison, the Eady configuration ($v = \infty$, $\lambda \neq \infty$) is shown in (d). The phase velocities are displayed in units of the non-dimensional height η of the interface. (In the lower layer this value corresponds to the steering level $[\bar{U} = u_p]$ of the mode.) The dashed curves refer to the surface mode (13) and interface mode (14), the dotted curve to the upper layer mode (15) (cf. Subsection 4.1).

3.2. *Role of the upper layer shear and stratification*

An overview of stability properties in the (ν, λ)-parameter space will be given in terms of four quantities: the maximum growth rate σ_M, the corresponding wave number γ_M and the wave numbers γ_S of the sort wave cut-off and γ_L of the long wave cut-off. (Note that wave modes with $\gamma_L < \gamma < \gamma_S$ are unstable.)

Fig. 2 displays these four characteristic quantities in (ν, λ)-space. For statically stable configurations ν is positive, whereas λ may achieve negative values if the shear in the upper layer is reversed. The dashed curve outlines the boundary of the parameter domain $\lambda \geqslant \nu^2$ where all wave lengths are baroclinically stable. In Fig. 2a, the maximum growth rates are smaller than that of the standard Eady (1949) problem ($\sigma_M^2 = 0.096$). For very large ν, however, a large upper layer shear causes a very unstable potential vorticity structure and produces maximum growth rates that exceed Eady's value (by one sixth for $\lambda \approx 0.4\nu^2$, $\nu \to \infty$). The wave number γ_M (Fig. 2b) is smaller than the corresponding Eady quantity ($\gamma_M = 0.80$) in the parameter range $\lambda \geqslant -0.6\nu$ and larger elsewhere. Thus, sufficiently strong reversed shear in the upper layer shifts the maximum growth to shorter wavelengths. The wave number of the short-wave cut-off (Fig. 2d) increases in the clockwise direction and attains its Eady value ($\gamma_S = 1.20$) for $\lambda \approx -1.2\nu$. The long wave cut-off (Fig. 2c) appears in two distinct areas separated by a zone without long stable modes at $\lambda = 0$. The higher the absolute value of the shear in the upper layer, the larger is γ_L.

The behaviour of different wavelengths for a few selected model configurations is depicted in Fig. 3. It displays the square of the growth rate σ^2 and the phase velocity u_p. In the stable wavelength interval there exist two neutral modes with distinct phase velocities related to the two solutions

$$\omega_{\pm} = b \pm \sqrt{(b^2 - c)}. \tag{12}$$

of eq. (8). In the lower model layer the non-dimensional shear of the basic wind is unity and thus the value of u_p indicates directly the height of the steering level at which the phase velocity equals the wind speed. Fig. 3a–c show that the phase velocity of the unstable modes increases with λ and, for the given configurations, is always larger than in Eady's case (Fig. 3d).

Table 1. *Parameter changes in the lower layer; listed is the qualitative influence of an increase in either the stratification N_l or the shear Λ_l of the lower layer on the maximum growth rate σ_M, the related wave number k_M and the wave numbers of the short wave cut-off k_S and of the long wave cut-off k_L (non-normalized, dimensional quantities)*

		σ_M	k_M	k_S	k_L
$N_1 \uparrow$	$\Lambda_2 > 0$	↓	↓	↓	↑
	$\Lambda_2 < 0$	↓	↓	↓	↓
$\Lambda_1 \uparrow$	$\Lambda_2 > 0$	↑	↑	↑	↓
	$\Lambda_2 < 0$	↑	↓	↓	↓

Fig. 3b displays the absence of a long wave cut-off in the case no upper layer shear. Adding a rigid upper lid to such a configuration (Bell and White, 1988) produces a significant increase of both the maximum growth rate and the related wave number, removing both lids (James and Hoskins, 1985) causes smaller values than in our case. Thus the present approach constitutes the intermediate state between these two models.

The situation for a case of constant shear in both layers, but varying stratification is depicted in Fig. 3c. In his original work Eady (1949) made a short reference to this structure and Blumen (1979) examined it for an additional upper rigid lid. This latter feature generates a third wave mode and, for some cases, splits the unstable wave number interval. Comparable results are presented by Nakamura (1988) for a continuous transition between the layers. Thus the introduction of a rigid lid in our model causes substantial qualitative changes. The maximum growth rates, however, are of the same order of magnitude.

3.3. *Influence of the lower layer*

So far our considerations were focussed on variations of the shear and stratification in the upper layer. To complete the picture, Table 1 displays qualitatively the influence of an increase in either the stratification or the shear of the lower layer. (Since such changes influence the conversion to non-dimensional quantities dimensional values are examined.) It is apparent that a reduction of N_1 as well as an increase of Λ_1 cause an amplification of the instability. The impact on the three characteristic wave numbers is more complex because it is also determined by the direction of the shear in the upper layer.

4. Wave characteristics

In the following the characteristic structures and wave properties of the long and short neutral modes and of the unstable modes will be examined and related to the structure of the basic potential vorticity, the vertical structure of the modes and their phase velocities.

4.1. Neutral modes

Examples of the vertical amplitude distribution of short neutral modes are given in Figs. 4a, b. The ω_+ mode (Fig. 4a) is concentrated at the interface

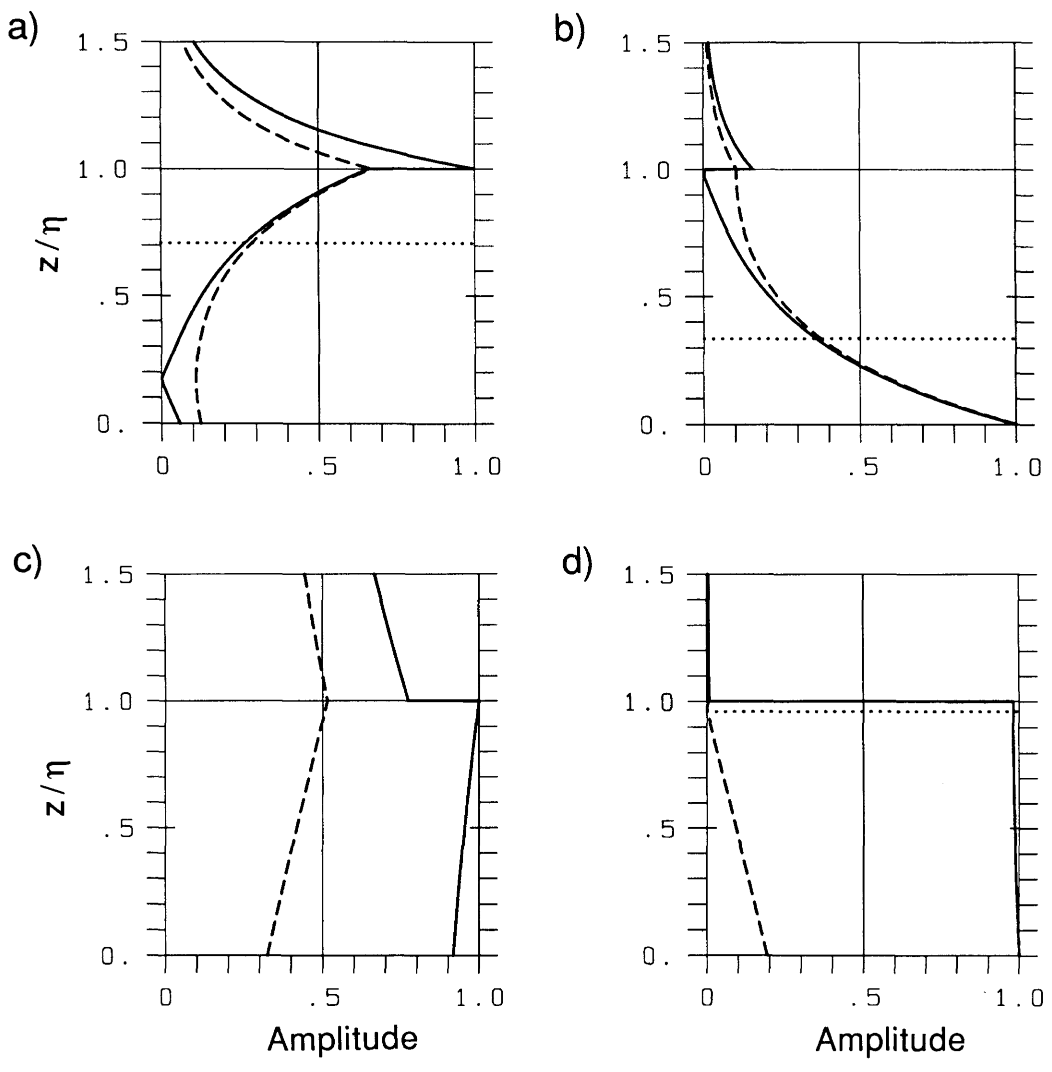

Fig. 4. Amplitude changes with height of the potential temperature θ' (solid) and the northerly wind v' (dashed curve) for neutral modes. Both amplitudes have been normalized with the maximum temperature amplitude of the respective case and z is given in units of the height η of the interface. Shown are (a) ω_+ and (b) ω_- for $v = 1.5$, $\lambda = 0$, $\gamma = 1.5$ and (c) ω_+ and (d) ω_- for $v = 1.5$, $\lambda = -1$, $\gamma = 0.1$. The dotted curve indicates the height of the steering level.

and the ω_- mode (Fig. 4b) at the surface, where the indices + and − refer to the two different neutral modes (12). In essence such modes do not "feel" simultaneously the two sheets of the potential vorticity gradient at the surface and the interface. Thus, they are stable, although the necessary condition for instability (11) is fulfilled. Figs. 4c, d display examples of the vertical structure of long neutral modes. The amplitude of the ω_- mode (Fig. 4d) is confined to the lower layer where its temperature is almost constant. Its counterpart, the ω_+ mode (Fig. 4c), exhibits large amplitudes in the upper layer.

Now consider the asymptotic behaviour of the neutral modes. For very short modes, the phase speeds are approximated by

$$u_{\mathrm{p}^+} \to \eta\left(1+\frac{\lambda-\nu^2}{2\nu(\nu+1)}\frac{1}{\gamma}\right)$$

$$\text{in the limit} \quad \gamma \to \infty \tag{13}$$

$$u_{\mathrm{p}^-} \to 1/k = \eta/(2\gamma)$$

$$\text{in the limit} \quad \gamma \to \infty, \tag{14}$$

and for very long waves the phase speeds are

$$u_{\mathrm{p}^+} \to \eta\left(\frac{\lambda}{2\nu}\frac{1}{\gamma}+1-\lambda\right) \qquad \text{for} \quad \gamma \to 0 \tag{15}$$

$$u_{\mathrm{p}^-} \to \eta \qquad \text{for} \quad \gamma \to 0. \tag{16}$$

Fig. 3 depicts the expressions (13, 14) by dashed curves and (15) by a dotted curve.

In the short wave limit both modes propagate eastward and their critical levels approach the surface and the interface. They will be called "interface mode" (Fig. 4a, eq. (13)) and "surface mode" (Fig. 4b, eq. (14)), respectively. In particular the "surface mode" propagates as if the model consisted only of one layer with uniform vertical structure. (Some implications of this special phase relationship on atmospheric frontogenesis are discussed by Müller et al. (1989).) In effect the short neutral modes are determined by external or internal fluid boundaries.

The long neutral modes are controlled by either of the two layers. The "upper layer mode" (Fig. 4c, eq. (15)) corresponds to a one-layer model with shear λ and stratification ν. This wave penetrates deep into the upper layer (3.3η for the example shown in Fig. 4c) and therefore ignores the lower layer. The direction of propagation is determined by the sign of λ (eastward for a positive value). The "lower layer mode" (Fig. 4d, eq. (16)) is the solution of a model with uniform shear and stratification in the entire atmosphere ($\nu = 1$, $\lambda = 1$), if an interface permits a kink in the geopotential field. Thus the thermal field may be trapped in the lower layer.

The stability of the neutral modes can of course be influenced by physical processes or variations in the third dimension that are neglected in our model. For example, the β-effect can favour short-wave instability and the occurrence of long neutral modes, but compressibility can compensate its effect (Read, 1988). In the long wave limit an adjustment of the meridional extension of the mode also diminishes the role of the β-effect (Hoskins and Revell, 1981). Weng and Barcilon (1987) found in a two-layer model that Ekman dissipation and heating cause growth in the short wave band. In isolation each of these effects exerts a significant influence on the stability characteristics, but it is also to be noted that they partly counteract and hence the overall impact may be comparatively small.

4.2. *Unstable waves*

Vertical amplitude distributions for unstable modes are illustrated in Fig. 5. The panels (a)–(c) show the same model configuration near the short wave cut-off, for the maximum growth rate and near the long wave cut-off. The amplitudes attain significant values at both the surface and the interface, i.e., at the levels with different signs of the potential vorticity gradient (10). Such a pattern supports instability. The amplitude minimum in the two layer is reached slightly above the steering level.

The phase shift with height of the most unstable mode is shown in Fig. 5d. At the level of minimum amplitude (cf. Fig. 5b) the phases of the θ'- and v'-fields coincide. The phase of the geopotential (identical with the phase of v') slants westward. This phase difference between the surface and the interface is related directly to the instability (cf. the conceptual appraoch to potential vorticity dynamics outlined in Hoskins et al. (1985)): The perturbations at the interface and surface are translated relative to each other such that their respective wind fields help to maintain these positions while they propagate in the sheared flow.

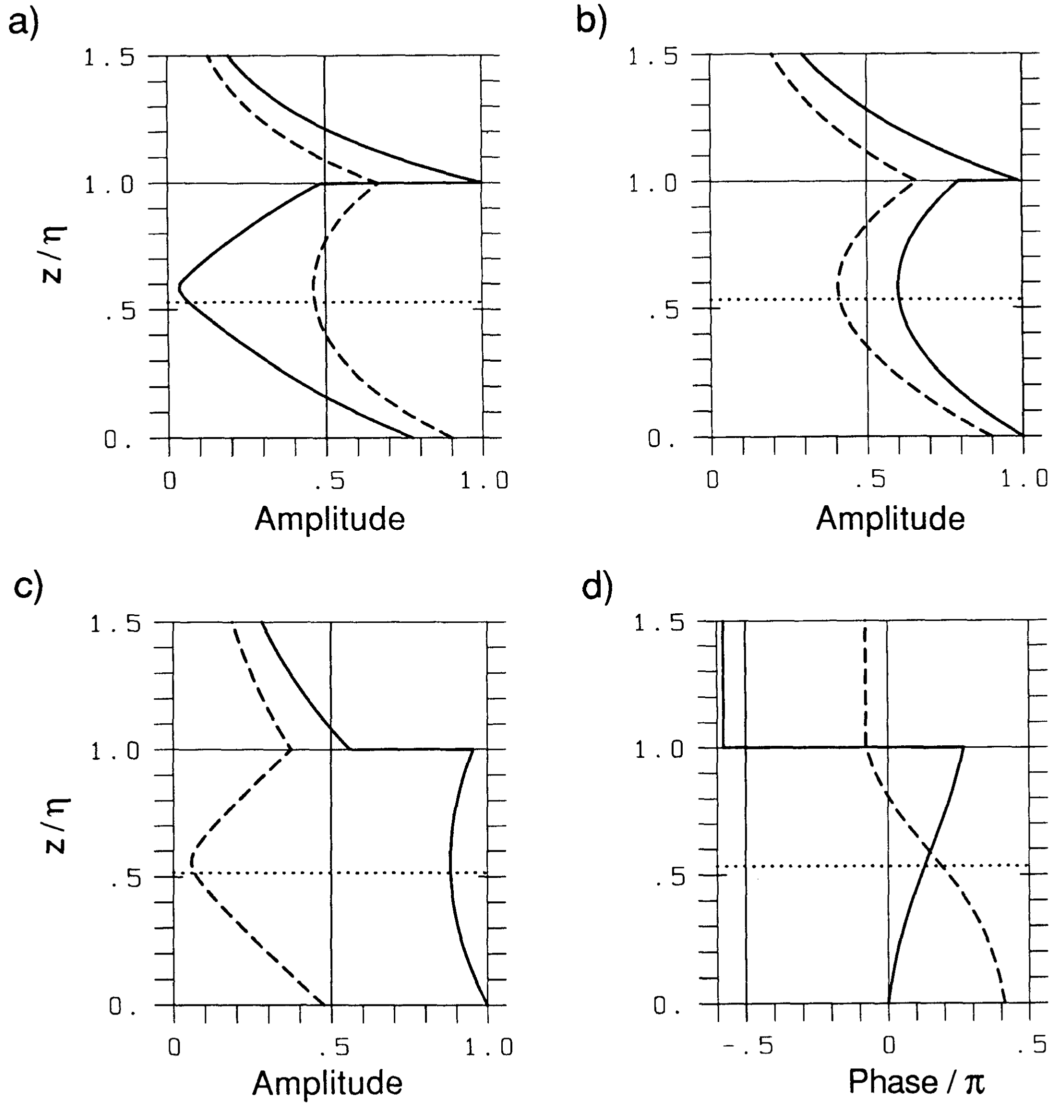

Fig. 5. Vertical structure of unstable modes. The basic state configuration is $v = 1.5$, $\lambda = -1$. Wave amplitudes are shown for (a) $\gamma = 1.10$, (b) $\gamma = 0.81$, (c) $\gamma = 0.46$ and (d) the phase shift with height (in units of π) for $\gamma = 0.81$ (cf. b). All other conventions are as in Fig. 4.

Such a phase lock leads to a mutual amplification of the perturbation.

This phase correlation is now examined in more detail. At the wave number γ_P $\{=(2v^2+v-\lambda)/(2v[v+1])\}$ the phase speeds of the interface (13) and surface modes (14) coincide and the perturbations at the sheets of non-zero potential vorticity gradient (10) propagate in phase. It can be shown that for all basic flow configurations supporting baroclinic instability

$$\gamma_M < \gamma_P < \gamma_S, \tag{17}$$

i.e., modes with the wave number γ_P are always unstable. This fact is remarkable for negative λ and sufficiently large v (lower left corner in Fig. 2) because then a rather narrow band of short unstable modes appears. The instability occurs although the vertical extent of the interface and surface modes are small. However, their virtually coinciding phase speeds provide the possibility of coupling of the modes. (An analogous argument applies for configurations with significant growth rates). Such short unstable waves were also obtained by Blumen (1979), Weng and Barcilon (1987) and Nakamura (1988) but, on account of an additional upper rigid lid, they found a second growth rate maximum at longer wavelengths. The occurrence of a long unstable mode near $\lambda = 0$ (cf. Fig. 3b) can be explained by a similar argument. In this parameter domain the phase velocities of the upper and lower layer modes (15, 16) coincide, the modes couple and baroclinic growth is produced.

5. Further remarks

A balanced flow model with different shear (or baroclinicity) and stratification in two layers was examined for baroclinic instability. The semi-infinite model domain can be viewed as representing an idealized troposphere-stratosphere structure, or two layers in the troposphere, or in a deep ocean (for z reversed). The dispersion and structure of two-dimensional wave modes was studied for arbitrary basic flow parameters.

Three wave length ranges were found with characteristic behaviour: Short and long modes are neutral and in an intermediate interval, baroclinic growth is produced. The present model provides us with results relating to:

- the role of upper layer shear: strong upper layer shear causes stability (cf. the necessary condition for instability), reversed shear allows for short wave instability and non-zero shear produces long neutral modes;
- neutral modes: the characteristics of the short modes are determined by an external or an internal fluid boundary and those of the long modes by one or other of the layers;
- baroclinic instability: large depth of the waves is not sufficient for instability; the modes have to propagate at a similar velocity that an interaction of perturbations at the sheets of non-zero potential vorticity gradient is possible; for shallow modes this mechanism can even produce instability in the short wave band;
- the role of a rigid lid: the classical model of Eady (1949) is contained in the present approach for infinite static stability in the upper layer; in the two-layer configuration, however, larger growth rates with a maximum at longer waves can occur for a very stable, sheared upper layer; a rigid upper lid is not required for the generation of rapid baroclinic growth.

An application of the results to rapid cyclogenesis and in particular to the formation of polar lows is attempted. Harrold and Browning (1969) explained this latter process as a baroclinic disturbance and attributed its small horizontal scale to a shallow vertical extension of the baroclinic zone. The hypothesis was supported by results from a shallow Eady-type model (Mansfield, 1974). The polar lows described by Reed (1979), however, formed in baroclinic fields that extended throughout the troposphere. Such a deep structure can be simulated with the present model. Consider the interface to be chosen at a low level, and we assume a baroclinic field in the upper layer such that $\lambda > 0$. The maximum growth rate is not affected by the lower layer depth, but the corresponding wave length is proportional to H. Now the static stability N_1 is decreased and according to Table 1 the growth rate rises whereas the length of the most unstable mode diminishes further. Thus the present model allows the scale reduction of the fastest growing mode in two complementary steps. The required pattern of a shallow layer with small static stability corresponds to observations (Reed, 1979).

The two-layer model examined in this study owes its analytical simplicity to the absence of an upper rigid lid and the two-dimensionality of the perturbations. Some restrictions arise from this idealized structure and from the omission of various physical processes. For example Robinson (1989) considered the dynamical importance of potential vorticity/β-effects at low levels and his results indicate that these ingredients can surpass the contribution of the tropopause. This conclusion, however, applies to an unbounded atmosphere with β-effect. The present model provides useful insight on the wave dynamics of a basic two-layer flow system and the results can be exploited to examine some atmospheric/oceanographic flow features.

REFERENCES

Bell, M. J. and White, A. A. 1988. The stability of internal baroclinic jets: Some analytical results. *J. Atmos. Sci. 45*, 2571–2590.

Blumen, W. 1979. On short-wave baroclinic instability. *J. Atmos. Sci. 36*, 1925–1933.

Bretherton, F. P. 1966. Critical layer instability in baroclinic flows. *Quart. J. Roy. Meteor. Soc. 92*, 325–334.

Eady, E. T. 1949. Long waves and cyclone waves. *Tellus 1*, No. 3, 33–52.

Harrold, T. W. and Browning, K. A. 1969. The polar low as a baroclinic disturbance. *Quart. J. Roy. Meteor. Soc. 95*, 710–723.

Hoskins, B. J. and Revell, M. J. 1981. The most unstable long wavelength baroclinic instability modes. *J. Atmos. Sci. 38*, 1498–1503.

Hoskins, B. J., McIntyre, M. E. and Robertson, A. 1985. On the use and significance of isentropic potential vorticity maps. *Quart. J. Roy. Meteor. Soc. 111*, 877–946.

James, I. N. and Hoskins, B. J. 1985. Some comparisons of atmospheric internal and boundary baroclinic instability. *J. Atmos. Sci. 42*, 2142–2155.

Mansfield, D. A. 1974. Polar lows: The development of baroclinic disturbances in cold air outbreaks. *Quart. J. Roy. Meteor. Soc. 100*, 541–554.

Müller, J. C., Davies, H. C. and Schär, C. 1989. An unsung mechanism for fronto- and cyclogenesis. *J. Atmos. Sci. 46*, 3664–3672.

Nakamura, N. 1988. Scale selection of baroclinic instability — effects of stratification and nongeostrophy. *J. Atmos. Sci. 45*, 3253–3267.

Pedlosky, J. 1987. *Geophysical fluid dynamics.* 2nd edition Springer, New York, 710 pp.

Read, P. L. 1988. On the scale of baroclinic instability in deep, compressible atmospheres. *Quart. J. Roy. Meteor. Soc. 114*, 421–437.

Reed, R. J. 1979. Cyclogenesis in polar air streams. *Mon. Wea. Rev. 107*, 38–52.

Robinson, W. A. 1989. On the structure of potential vorticity in baroclinic instability. *Tellus 41A*, 275–284.

Simmons, A. J. 1979. Baroclinic instability and frontogenesis. *Dynamical Meteorology and Numerical Weather Prediction*, ECMWF Seminar 1979, Volume I, 34–174.

Weng, H. Y. and Barcilon, A. 1987. Favorable conditions for explosive cyclogenesis in a modified two-layer Eady model. *Tellus 39A*, 202–214.